

# Concentration Dependence of Optical Properties in Arsenic-Doped ZnO Nanocrystalline Films Grown on Silicon (100) Substrates by Pulsed Laser Deposition

W. W. Li,<sup>†</sup> Z. G. Hu,<sup>\*,†</sup> J. D. Wu,<sup>‡</sup> J. Sun,<sup>‡</sup> M. Zhu,<sup>\*,§</sup> Z. Q. Zhu,<sup>†</sup> and J. H. Chu<sup>†</sup>

Key Laboratory of Polar Materials and Devices, Ministry of Education, East China Normal University, Shanghai 200241, People's Republic of China, State Key Laboratory for Advanced Photonic Materials and Devices, Department of Optical Science and Engineering, Fudan University, Shanghai 200433, People's Republic of China, and Department of Physics, Shanghai Jiao Tong University, Shanghai 200240, People's Republic of China

Received: March 27, 2009; Revised Manuscript Received: August 24, 2009

Arsenic (As)-doped (1% to 3%) ZnO nanocrystalline films with the grain size of 20 nm have been grown on silicon substrates by pulsed laser deposition. X-ray diffraction analysis shows that the films are polycrystalline and exhibit the hexagonal wurtzite phase. The As dopant effects on lattice vibrations and electronic transitions of the ZnO films have been investigated by Raman scattering and photoluminescence spectra at room temperature. With increasing As concentration,  $A_1(\text{LO})$  phonon frequency is shifted toward lower energy side of  $4 \text{ cm}^{-1}$ . Ultraviolet and near-infrared optical transitions can be observed and remained as a constant. Moreover, orange and green luminescence are strongly dependent on the As concentration owing to different oxygen vacancy, zinc vacancy, oxygen interstitial, and morphology. Dielectric functions of the films have been determined in the photon energy from 2.5 to 6.0 eV by near-normal incident spectral reflectance. By fitting the experimental data with the Adachi's model, [Adachi, *S. Phys. Rev. B* **1987**, 35, 7454] the optical constants and film thickness have been uniquely extracted. It is found that the dielectric function values of the films are less than that of undoped ZnO material, which could be attributed to the As doping and the porosity of films.

多孔性

## I. Introduction

Zinc oxide (ZnO) is an important direct wide-band gap semiconductor (WBGs), which is very similar to gallium nitride (GaN) in both crystal structure and optical properties. For several decades, much effort has been made on the studies of ZnO with regard to its potential technological applications in photodetectors, light emitting diodes, and laser diodes due to its wide band gap (3.37 eV) and large exciton binding energy of 60 meV at room temperature (RT).<sup>1–12</sup> One of the important steps for the development of ZnO-based devices is to fabricate stable and high quality *n*-type and *p*-type ZnO materials. It is widely recognized that in all WBGs only one type of doping, either *n*-type or *p*-type, is easily achieved.<sup>11</sup> The fabrication of high crystalline quality *n*-type ZnO, which is sufficiently good for device applications, has been already realized. Unfortunately, the growth of *p*-type ZnO films is rather difficult because of its self-compensation effect, deep acceptor level, and low solubility of dopants.<sup>13–15</sup> Many research groups have focused on the fabrications of *p*-type ZnO films by group V element doping, such as nitrogen (N), phosphorus (P), and arsenic (As).<sup>6–8</sup> In particular, some attentions have been drawn to As element doped ZnO (ZnO:As) films.<sup>8–10</sup> This is because As can be regarded as an alternative acceptor with both low formation energy and low ionization in ZnO material. Furthermore, it is easy to realize the high solubility of As by some appropriate doping methods.<sup>8–10</sup> Although there are some studies on the growths of ZnO:As material, the As dopant effect on its optical properties, which is one of the crucial issues for the optoelectronic applications

of ZnO semiconductor, is still scarce and needs more investigations.

As we know, the physical properties of nanocrystalline films are strongly dependent on substrate, growth technique, crystalline quality, intrinsic defects and doping elements.<sup>13,14</sup> Many fabrication techniques are currently applied to prepare ZnO:As films such as pulsed laser deposition (PLD),<sup>8</sup> hybrid beam deposition,<sup>4</sup> and chemical vapor deposition.<sup>15</sup> Among them, PLD is a well-adopted method due to its evident advantages such as high quality of film, composition control and uniformity. For *p*-type ZnO material, the As concentration ( $C_{\text{As}}$ ) is an important factor for ZnO:As compound because the As dopant can induce more mismatches and defects in the lattice structure, which can affect its electronic band structures and optoelectronic properties. Jeong et al. found that the  $E_2^{\text{high}}$  phonon mode of ZnO:As films has a blueshift of about  $0.55 \text{ cm}^{-1}$ , as compared with that of undoped ZnO bulk crystal.<sup>3</sup> Wahl et al. suggested that the As atom does not occupy substitutional O sites but in its large majority substitutional Zn sites.<sup>11</sup> Ryu et al. reported that the peak positions of luminescence are shifted to lower energy side with increasing  $C_{\text{As}}$ .<sup>4</sup> In spite of the promising properties, there are no systematical reports on concerning the relationship among lattice vibrations, ultraviolet, visible and near-infrared (NIR) luminescence, and the As concentration for ZnO:As films.

The optical constants play an important role in the optoelectronic device design. For example, energy transport by exciton and performance of luminescent devices depends on the dielectric constant of the concerned material.<sup>16</sup> Furthermore, dielectric function can be directly related to the electronic band structure of material.<sup>17</sup> Although there are some reports on the dielectric functions of ZnO single crystals and films,<sup>16,18,19</sup> up to date, the dielectric properties of ZnO:As films with different

\* Corresponding authors. E-mail: zghu@ee.ecnu.edu.cn; zhumin@sjtu.edu.cn.

<sup>†</sup> East China Normal University.

<sup>‡</sup> Fudan University.

<sup>§</sup> Shanghai Jiao Tong University.

$C_{As}$  have not been studied. In order to elucidate the distinguishing physical behavior and further exploit the material as a viable candidate for fabricating ZnO-based optoelectronic devices, the As-related optical properties should be thoroughly investigated. There are some spectral techniques to determine optical constants of film materials on oblique substrates. Among them, spectroscopic ellipsometry (SE) and reflectance spectra are easily acceptable for the determination of optical constants. Although SE is a standard method to measure optical function of a multilayer system without the Kramers–Krönig transformation (KKT) due to determining two independent angles simultaneously,<sup>20</sup> the optical model selection and fitting calculation in SE experiments can be more complicated as compared with reflectance spectra.<sup>21</sup> Optical reflectance technique is an attractive and powerful tool for the optical characterization of semiconductor film materials, which can directly provide electronic band energy and dielectric constants. Moreover, spectral reflectance have been successfully applied to obtain optical functions of semiconductor and dielectric materials.<sup>22–24</sup> Note that the KKT in reflectance spectra is only valid for a wider photon energy owing to the rigorous condition for the total light frequency integral. Thus, to reasonably interpret reflectance spectra measured in the limited photon energy range, a dielectric function model can be uniquely selected to reproduce the experimental data.<sup>25,26</sup>

In this paper, the structure, lattice vibrations and photoluminescence (PL) properties of ZnO:As films deposited on silicon (100) substrates with different  $C_{As}$  have been studied. The dielectric function from ultraviolet (UV) to visible photon energy region of the films has been investigated using reflectance spectra. A theoretical model is presented to fit the experimental reflectance spectra. The effects from the As dopant on the optical properties have been discussed in detail.

## II. Experimental Details

**Fabrication of the ZnO:As Films.** Nanocrystalline ZnO:As films with the thickness of about 900 nm were grown by PLD in an oxygen rich (O-rich) ambient. The targets were made from the mixtures of high purity ZnO and  $As_2O_3$  powders. Using  $As_2O_3$  other than ZnAs as dopant is due to the fact that  $As_2O_3$  is more beneficial to the formation of  $As_{Zn}$  (As occupy the site of Zn) than that of  $As_O$  (As occupy the site of O). The high solubility of the As element can be easily obtained by the method because of the ratio of  $As_2O_3/ZnO$  that can be freely manipulated in preparation of the ZnO/ $As_2O_3$  target. The  $As_2O_3$ -mixed ZnO targets were prepared by a conventional process for ceramic power. The ZnO:As films were grown on intrinsic silicon (100) substrates at a substrate temperature of 450 °C and an  $O_2$  pressure of 5 Pa. The growth chamber was pumped down to a base pressure of  $10^{-4}$  Pa prior to backfilling it with the ambient  $O_2$ . A pulsed Nd:YAG (yttrium aluminum garnet) laser (532 nm wavelength, 5 ns duration) operated with an energy of 60 mJ/pulse and repetition rate of 10 Hz was used as the ablation source. The distance between the target and the substrate was kept at 3 cm. The deposition time was usually set to about 30 min. The As atom concentration of the ZnO:As films is kept at 1%, 2%, and 3%, respectively, which is confirmed by X-ray photoelectron spectroscopy (XPS) experiments. The detailed growth process can be found in ref 8.

**XRD, AFM, Raman, PL, and Reflectance Spectral Measurements.** The crystalline structure of the ZnO:As films was analyzed by X-ray diffraction (XRD) using Cu  $K\alpha$  radiation (D/MAX-2550 V, Rigaku Co.). The surface morphology was investigated by atomic force microscopy (AFM; Digital Instru-

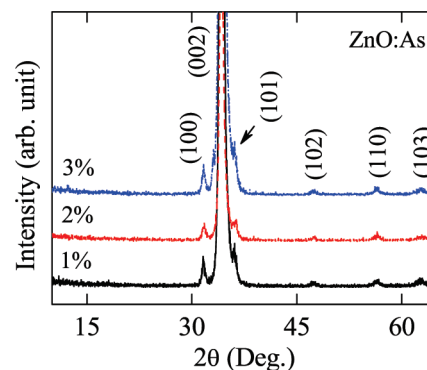


**Figure 1.** XRD patterns of the ZnO:As films grown on Si substrates with different As concentrations of 1%, 2%, and 3%, respectively. Note that the (002) diffraction peak is cut because of much stronger intensity.

ments Dimension 3100, Veeco). From the AFM pictures, the average grain size can be evaluated to about several tens nanometers. It can be concluded that the ZnO:As films are of nanocrystalline growth mode (not shown). Raman scattering experiment was done by a Jobin-Yvon LabRAM HR 800 UV micro-Raman spectrometer using resonant Raman spectral method with a He–Cd laser as the excited light, which is operated at the wavelength of 325 nm (3.82 eV).<sup>13</sup> PL spectra were recorded with the same spectrometer and laser source with the excitation power (EP) of 30 mW. Incident EP was controlled by the calibrated neutral density filters in the front of the spectrometer slit. In the experiments, the laser beam EP on the sample surface can be roughly tuned from 0.3 mW to 30 mW. The optical reflectance measurements were done with a double beam ultraviolet–infrared spectrophotometer (Perkin Elmer Lambda 950) at the photon energy from 2.5 to 6.0 eV (208–496 nm) with a spectral resolution of 2 nm. Aluminum (Al) mirror, whose absolute reflectance was directly measured, was taken as reference for the spectra in the photon energy region. The reflectance spectra were recorded by universal reflectance accessory (URA). The angle of incidence is 8°. The samples were at room temperature for all measurements and no mathematical smoothing has been performed on the experimental data.

## III. Results and Discussion

**Structural Analysis.** The XRD patterns of the ZnO:As films with different  $C_{As}$  deposited on Si wafers are shown in Figure 1. As we can see, all three samples exhibit a single phase with the hexagonal wurtzite structure. The strongest diffraction peak appears near 34°, which is from the ZnO (002) plane. Compared with the results of undoped ZnO film,<sup>8</sup> several other weaker peaks (100), (101), (102), (110), and (103) are present. It indicates that the polycrystalline grains with different orientations were formed in the ZnO:As films. It confirms that the As atom has been successfully incorporated into the ZnO matrix lattice. Note that these results are slightly different from the single crystalline films on sapphire substrate.<sup>10</sup> It can be concluded that the crystallinity was changed due to the As atom incorporation. According to Scherrer's equation, the average grain size from the (002) peak of the ZnO:As samples is estimated to about 20 nm, which agrees well with those from the AFM experiments. Moreover, the present ZnO:As films grown on silicon (100) substrates could be optically isotropic owing to the polycrystalline formations and the near-normal incident light spot of about 5 mm in diameter.

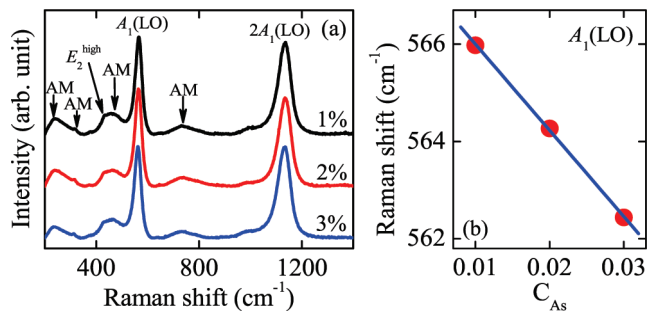


**Figure 2.** (a) Raman spectra of the ZnO:As films with different As concentrations under the excitation line of 325 nm. Note that the abbreviation “AM” denotes additional mode, and the spectra are vertically shifted for clarification. (b) The  $A_1(\text{LO})$  phonon mode shows a linear redshift trend with the As concentration.

**Lattice Vibrations.** Figure 2a shows lattice vibrations of the ZnO:As films with different As doping concentrations. It further indicates that the ZnO:As samples have the pure wurtzite structure. The  $E_2^{\text{high}}$  phonon mode, which is associated with the band characteristic of the wurtzite phase, can be observed at the infrared frequency of about  $428 \text{ cm}^{-1}$ . The weak scattering intensity could be due to the experimental configuration, which can give different Raman-active phonon mode information. The value is slightly less than that reported for the single crystal.<sup>27</sup> This discrepancy can be ascribed to different doping method and crystalline orientation. In addition, some additional modes (AM) located at about 236, 315, 468, and  $730 \text{ cm}^{-1}$  are the vibrations owing to the multiple-phonon scattering process.<sup>3</sup> The stress-induced effects from the lattice mismatch with the substrate may be responsible for these observed vibration modes.<sup>1</sup> Note that these values are slightly different from those of N doped ZnO films.<sup>28</sup> The phenomena can be ascribed to different atomic radius of dopants, surface damage, and crystalline quality of the samples.

The first sharp and intense peak can be assigned to the  $A_1$  longitudinal optical (LO) phonon mode. Note that the two  $A_1(\text{LO})$  phonon modes, which are related to second-order response of the  $A_1(\text{LO})$  phonon mode, can be also observed because Raman spectra were recorded under resonant measurement condition. With increasing  $C_{\text{As}}$ , it is worth noting that the  $A_1(\text{LO})$  phonon mode shifts toward the lower energy side and is located at about 566, 564, and  $562 \text{ cm}^{-1}$ , respectively. The result is in good agreement with the previous report in ref 21. Figure 2b shows the linear variation trend of the  $A_1(\text{LO})$  phonon mode with the  $C_{\text{As}}$ . The redshift of the  $A_1(\text{LO})$  phonon mode can be attributed to the increment of free carrier concentration with increasing  $C_{\text{As}}$ , which resulted in the increased frequency of LO–plasmon coupling modes.<sup>8,27</sup> Moreover, the intensity of the  $A_1(\text{LO})$  phonon mode decreases with increasing As concentration. With increasing  $C_{\text{As}}$ , the crystallinity can be deteriorated due to the increments of surface and lattice damage. Therefore, the degraded crystalline properties will induce the intensity of the  $A_1(\text{LO})$  phonon mode decreasing.<sup>3,28</sup>

**Photoluminescence Spectra.** In order to elucidate the  $C_{\text{As}}$  effects on the optical properties of the ZnO:As films, PL spectra are presented in Figure 3. The UV luminescence peak originating from free excitonic emission can be observed at about 3.22 eV, which is smaller than that reported by Ryu et al.<sup>4</sup> The full width at half-maximum of the UV peak is about 93 meV, which indicates that the films are of high crystal quality again. Note that a shoulder peak appears at about 3.12, 3.15, and 3.02 eV, respectively, which may be related to the first LO–phonon replica of the electron-acceptor (FA) transition and/or a neutral-

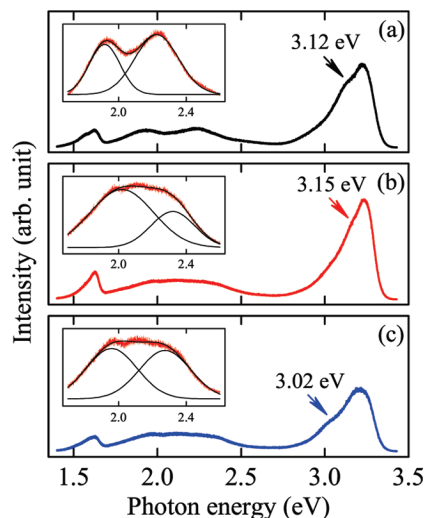


**Figure 3.** PL spectra of the ZnO:As films with different As concentrations of (a) 1%, (b) 2%, and (c) 3%, respectively. The insets show an enlarged visible photon energy region of 1.7–2.6 eV with the Gaussian model fitting.

acceptor-bound ( $A^0X$ ).<sup>29–31</sup> The intensity of visible and NIR luminescence is weaker, as compared with the UV emission. The shape of the visible band indicates that it should consist of more than one luminescence peak. The decomposition of the visible band in the photon energy range of 1.7–2.6 eV by the Gaussian curve fitting can be seen in the insets of Figure 3. Obviously, green luminescence (GL) can be observed at about 2.23, 2.32, and 2.28 eV, respectively, while orange luminescence (OL) is located at about 1.92 eV, 2.02 eV, and 1.96 eV, respectively. It should be emphasized that the visible band of the ZnO:As film with the As concentration of 3% may contain the third peak. However, in order to compare with the other samples, two luminescence peak analysis are still applied in the present work. The positions of both GL and OL has a slightly change with the  $C_{\text{As}}$ . The relatively (GL/OL) integrated intensity is 0.86, 0.86, and 0.87, respectively. It indicates that the defect centers for generating the two PL peaks are different and compete with each other. It was reported that a NIR luminescence peak, which is ascribed to the second-order diffraction of the UV emission, can be observed only in the films with a strong UV luminescence.<sup>32</sup> The phenomenon can be reproduced in the present ZnO:As films. For all three samples, a weak NIR peak can be observed at about 1.62 eV. Moreover, the NIR peak shape is similar to that of the UV peak. Interestingly, there is a shoulder characteristic from the NIR peak. It can be concluded that the ZnO:As films have much better optical properties.

Many reports have been given and have focused on the origin of the GL and OL in ZnO semiconductor. Early works suggested that the GL comes from oxygen deficient (O-deficient) while the OL comes from O-rich and not because of the amounts of dopants.<sup>33</sup> However, the present results indicate that both GL and OL can appear in O-rich ambience, and they are also related to the  $C_{\text{As}}$ . Recently, oxygen vacancy ( $V_{\text{O}}$ ) and zinc vacancy ( $V_{\text{Zn}}$ ) are considered to be responsible for the GL.<sup>5,32</sup> In the ZnO:As films, As substitutes on the Zn site, forming a donor, then it induces two  $V_{\text{Zn}}$  acceptors.<sup>9,11</sup> So, the  $V_{\text{Zn}}$  increases with the  $C_{\text{As}}$ . Moreover, it was reported that the peak of the (101) orientation was related to defects, such as  $V_{\text{O}}$ .<sup>34</sup> From the XRD results, the (101) diffraction peak is different from three ZnO:As films. So it can further affect the GL of the films. The yellow–orange emission is attributed to oxygen interstitial ( $\text{O}_i$ ) and associated with excess oxygen.<sup>33,35</sup> Along with As substi-



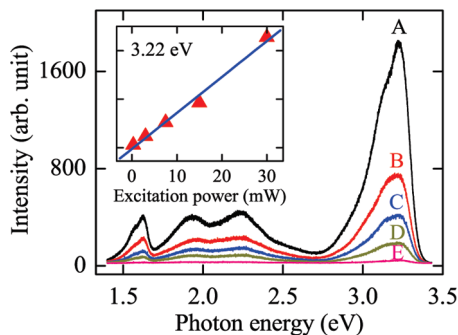


**Figure 4.** PL spectra of the ZnO:As film with the As concentration of 1% under different excitation power: (A) 30 mW, (B) 15 mW, (C) 7.5 mW, (D) 3 mW, and (E) 0.5 mW, respectively. The inset shows the ultraviolet peak intensity linearly increases with the excitation power.

tutes on the Zn site, the oxygen atom may leave the intrinsic site and settle in the interstitial site to form  $O_i$ . Additionally, it was found that the surface morphology of the ZnO:As nanocrystalline films is varied with different  $C_{As}$  from the AFM measurements. Kwok et al. reported that the sub-band emission in ZnO may associate with the nanostructure morphology.<sup>36</sup> So the surface morphology of the ZnO:As films plays an important role in the GL and OL. The influences of these factors on the GL and OL are competitive with each other. Therefore, we can conclude that the different green and orange emissions of the ZnO:As films are attributed to different  $V_o$ ,  $V_{Zn}$ ,  $O_i$ , and surface morphology. In order to clarify the phenomena, the PL properties at lower temperatures are necessary in the future work.

The EP dependence of PL spectra can provide the band-band and sub-band electronic transitions, which can give the generation and recombination probability of the excited free carriers in the valence, conduction band, and defect-related sub-bands. In order to obtain the above information for the ZnO:As films, the PL spectra as a function of the EP are plotted in Figure 4. As can be seen, all of the peak energy positions exhibit no change, and there are no additional luminescence peaks with different EP. All luminescence, especially for the GL and OL, become remarkably weak at the EP of 15 mW. Besides the strongest UV luminescence, some other emissions can hardly be seen with further decreasing EP. A linear variation trend has been found for the UV emission with different EP (see the inset of Figure 4). It is widely accepted that the PL intensity is generally increased with the EP. With increasing the EP, more carriers can be excited from the valence band and/or sub-band to the conduction band. Therefore, the recombination probability of electron-hole pair is increased and results in the strong emission peak. So, the PL intensity will present an increasing trend with the EP.<sup>1</sup> The experiment results indicate that the UV luminescence intensity increases linearly with the EP, which agrees well with above theoretical analysis.

**UV-visible Dielectric Function.** The inverse synthesis method is based on a phenomenological model fitted to the experimental results. A three-phase layered structure (air/film/substrate) was constructed for each sample to determine the optical properties of the ZnO:As films. The dielectric function of the substrates in the fitting can be taken from ref 31. For WBGs materials, the dielectric response, which can be described by the contribution from the lowest three-dimensional  $M_0$  type critical point (CP), is written as the following Adachi's model:<sup>21,38,39</sup>

$$\tilde{\epsilon}(E) = \epsilon_{\infty} + \frac{A_0[2 - (1 + \chi_0)^{1/2} - (1 - \chi_0)^{1/2}]}{E_g^{3/2} \chi_0^2} \quad (1)$$

here,  $\chi_0 = (E + i\Gamma)/E_g$ ,  $\epsilon_{\infty}$  is the high-frequency dielectric constant,  $E_g$  is the fundamental optical transition energy,  $E$  is the incident photon energy, and  $A_0$  and  $\Gamma$  are the strength and broadening parameters of the  $E_g$  transition, respectively. The above Adachi's model is successfully applied in many semiconductor and dielectric materials.<sup>12,13</sup> It should be emphasized that the dielectric function with the Adachi's model abides by the KKT in the entirely measured photon energy region.<sup>38,39</sup> The best-fit parameter values in eq 1 can be found by applying a Levenberg-Marquardt algorithm, which is an efficient nonlinear calculation method for many parameter fitting.<sup>41</sup> The fitting is based on minimizing the following error function:  $\chi = (1)/(N) \sum_{i=1}^n |R_{i,exp} - R_{i,cal}|^{2.25}$  where  $N$  is the number of experimental data points, and  $R_{i,exp}$  and  $R_{i,cal}$  are the experimental and calculation values, respectively.

The experimental reflectance spectra of the ZnO:As films at the incident angle of  $8^\circ$  are shown in Figure 5 with the dotted lines. All samples have a near-band-edge absorption in the photon energy range of 3.14 to 3.34 eV. An interference effect below the photon energy of about 3.2 eV, which is due to the multiple reflection between the film and the substrate, is clearly observed for all samples indicating that the films are transparent in this region. Note that the interference oscillation period for sample B grown at the  $C_{As}$  of 2% is less than the other two samples. This is because the film has the minimum thickness. The fitted parameters values in eq 1 and the fitted thicknesses are summarized in Table 1, and the simulated results with Adachi's model parameters are also shown in Figure 5 by the solid lines. A good agreement is obtained between the experimental and the fitted data in the entirely measured energy region. The high-frequency dielectric constant  $\epsilon_{\infty}$  of the ZnO:As films is varied from  $1.19 \pm 0.05$  to  $1.36 \pm 0.05$ , where those values are below the reported value for pure ZnO.<sup>19</sup> Generally, the parameter  $\epsilon_{\infty}$ , which is related to high-energy critical point transitions, accounts for the so-called high-frequency limit. Therefore, the dielectric function model should be extrapolated to shorter wavelengths than those studied here (up to 6.0 eV). It should be emphasized that the  $\epsilon_{\infty}$  variation of the ZnO:As films is not large, compared with the As doping concentration difference. The slight change might be a sign of significantly different morphologies of the different films because the shorter wavelength can be comparable to the surface rough layer thickness.

The evaluated dielectric functions of the ZnO:As films are shown in Figure 6. The evolution of  $\tilde{\epsilon}$  with the photon energy is a typical optical response behavior of dielectric and/or semiconductors.<sup>38-40,42</sup> Generally, the real part  $\epsilon_1$  increases with the photon energy and approaches the maximum, then decreases with further increasing photon frequency due to the known van Hove singularities.<sup>38,39,42</sup> The  $\epsilon_1$  value was approximately varied from 1.6 to 3.8 for all doping contents. In the wide transparent region, the imaginary part  $\epsilon_2$  is approximately down to zero. As the photon energy further increases, the  $\epsilon_2$  remarkably increases to about about 1.5 eV then slowly decreases up to the present measurement limitation (6.0 eV). It indicates that strong photon absorption appears, showing the fundamental band gap ( $E_g$ ) transition from the highest valence band to the lowest conduction band.<sup>19</sup> The excitonic absorption strongly affects the optical properties of ZnO near the edge.<sup>43</sup> It should be emphasized that the dielectric function values of our results are

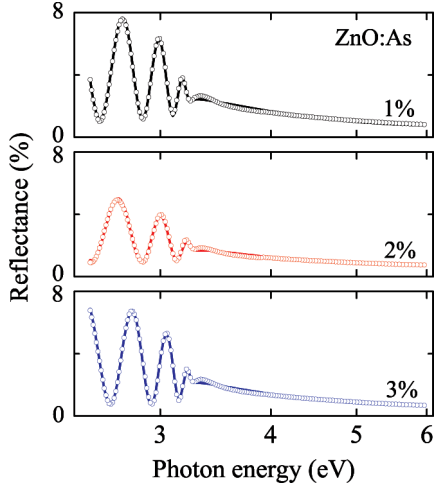


**Figure 5.** Experimental (dotted lines) and best-fit (solid lines) reflectance spectra of ZnO:As films from ultraviolet to visible photon energy region. The horizontal coordinate is the logarithmic unit to enlarge the transparent region.

**TABLE 1: Parameter Values of Adachi's Model for the ZnO:As Films with Different As Concentrations are Determined from the Simulation of Reflectance Spectra in Figure 5<sup>a</sup>**

samples	$C_{As}$	thickness $d$ (nm)	$\epsilon_\infty$	$A_0$ (eV <sup>3/2</sup> )	$E_g$ (eV)	$\Gamma$ (eV)
A	1%	910	1.36	26.7	3.24	0.04
		(17)	(0.05)	(1.1)	(0.05)	(0.01)
B	2%	823	1.19	26.2	3.27	0.06
		(12)	(0.05)	(1.1)	(0.01)	(0.01)
C	3%	888	1.28	27.6	3.25	0.05
		(16)	(0.06)	(1.1)	(0.01)	(0.01)

<sup>a</sup> The 90% reliability of the fitting parameters is given in parentheses.

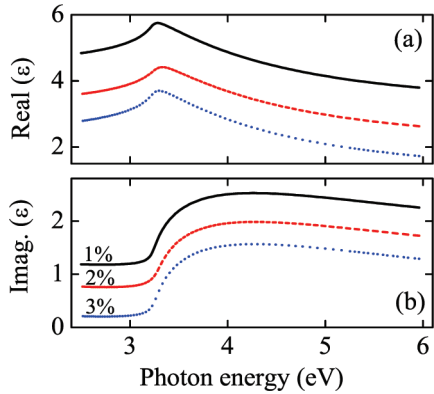


**Figure 6.** Arsenic concentration effects on the dielectric function (a) real part and (b) imaginary part for ZnO:As films in the photon energy range of 2.5–6.0 eV. Note that the  $\epsilon_1$  and  $\epsilon_2$  are vertically shifted by adding 1 and 0.5, respectively.

less than that previously reported on undoped ZnO,<sup>44,45</sup> which might be ascribed to the doping of As.

On the other hand, the porosity of films could be another possible cause because the increasing of porosity may induce more voids and less reflectivity. It is true that the ZnO:As film surface may be porous, and there are many voids on the sample surfaces from the AFM data. Generally, the porous surface layer could be several nanometers, which is much less than the film thickness. Nevertheless, the surface rough layer can be neglected owing to a smaller thickness value, whose contribution should be slight in the evaluation of the optical properties. In addition,

near normal-incident configuration is used in the present reflectance experiment, which indicates that the reflectance spectra cannot be sensitive to the thinner surface rough layer.<sup>21,22,37</sup> The Bruggeman effective medium approximation (BEMA) can be employed to explain this phenomenon, which is given by the following equation:<sup>46,47</sup>

$$f_A \frac{\tilde{\epsilon}_A - \tilde{\epsilon}}{\tilde{\epsilon}_A + 2\tilde{\epsilon}} + f_B \frac{\tilde{\epsilon}_B - \tilde{\epsilon}}{\tilde{\epsilon}_B + 2\tilde{\epsilon}} = 0 \quad (2)$$

Here,  $f_A + f_B = 1$ , where  $f_A$  and  $f_B$  are the volume fraction of voids and the ZnO:As film, respectively.  $\tilde{\epsilon}_A = 1$  is the dielectric function of air, and  $\tilde{\epsilon}_B$  is the dielectric function of the ZnO:As film. Because of the existence of voids, what we virtually obtained is the pseudodielectric function that co-operated by air and the ZnO:As film, which is less than that calculated from fully dense ZnO:As film. However, because the voids are an inhomogeneous distribution, the parameters of the model are considerably complex, and the workload of calculation is terrifically large, it is extremely difficult to extract  $f_A$  or  $f_B$ . From AFM results, one can also observe that the surface of the ZnO:As films are incompact and porous. Therefore, it can be concluded that the As doping and the existence of some voids may affect the dielectric function of the ZnO:As film. As previously discussed, the polycrystalline films are optically isotropic, which normally cannot result in the dielectric function decrement, as compared with undoped ZnO and its bulk crystal. It could be believable that the film inhomogeneity plays an important role in the decreasing of optical constants.

As we know, the depolarization effect can result in decreasing the reflectance of the films. The phenomena can make the above optical model unsuccessful if a stronger depolarization is induced by the film inhomogeneities for the reflectance spectra.<sup>20</sup> However, the present evaluation is still valid and acceptable because the ZnO:As films are not remarkably depolarized in view of a good fitting quality ( $\chi \sim 10^{-2}$ ) and logical spectral line shape, as seen in Figure 5. In addition, the smooth oscillator curve in the transparent region shows that the depolarization effects in the nanocrystalline films are not distinct and can be neglected. It indicates that the three-phase layered structure and the Adachi's dielectric function model are reasonable for the present ZnO:As nanocrystalline films. Note that calculating film inhomogeneity and nonideality is not successful because of the complicated many-parameter system in the present work. More sensitive polarized spectral measurement, such as SE and variable-angle polarized reflectance,<sup>21,26,37</sup> could be desirable to determine these physical properties of the ZnO:As films.

#### IV. Conclusion

To summarize, the As concentration dependence of the lattice vibrations and electronic transitions in the ZnO:As films has been investigated using Raman scattering and PL spectra. The  $A_1(\text{LO})$  and  $E_2^{\text{high}}$  phonon modes appear with the As incorporation. Luminescence peaks in the UV, green, orange, and NIR energy region can be well-observed, and the origin has been discussed. It was found that the GL and OL of the ZnO:As films can be strongly affected by the As doping concentration. The dielectric function of the films has been studied by spectral reflectance. The theoretical analysis based on the BEMA theory is well-used to explain these experimental data. The present results could be crucial for future applications of ZnO-based optoelectronic devices.

**Acknowledgment.** The authors would like to acknowledge professor X. D. Tang, Mr. J. Y. Zhu, and Dr. F. Y. Yue for the AFM experiments and technical supports. This work was financially sponsored by Major State Basic Research Development Program of China (Grant 2007CB924901), the Program of New Century Excellent Talents, Ministry of Education (Grant NCET-08-0192), and Shanghai Municipal Commission of Science and Technology Project (Grants 07PJ14034, 07JC14018, 07DZ22943, 08JC1409000, and 08520706100).

## References and Notes

- (1) Özgür, Ü.; Alivov, Ya. I.; Liu, C.; Teke, A.; Reshchikov, M. A.; Doğan, S.; Avrutin, V.; Cho, S.-J.; Morkoç, H. *J. Appl. Phys.* **2005**, *98*, 041301.
- (2) Fan, J. C.; Xie, Z.; Wan, Q.; Wang, Y. G. *J. Cryst. Growth* **2007**, *304*, 295.
- (3) Jeong, T. S.; Han, M. S.; Youn, C. J.; Park, Y. S. *J. Appl. Phys.* **2004**, *96*, 175.
- (4) Ryu, Y. R.; Lee, T. S.; Leam, J. H.; White, H. W. *Appl. Phys. Lett.* **2003**, *83*, 87.
- (5) Zhang, W. C.; Wu, X. L.; Chen, H. T.; Zhu, J.; Huang, G. S. *J. Appl. Phys.* **2008**, *103*, 093718.
- (6) Look, D. C.; Reynolds, D. C.; Litton, C. W.; Jones, R. L.; Eason, D. B.; Cantwell, G. *Appl. Phys. Lett.* **2002**, *81*, 1830.
- (7) Aoki, T.; Hatanaka, Y.; Look, D. C. *Appl. Phys. Lett.* **2000**, *76*, 3257.
- (8) Shen, Y. Q.; Hu, W.; Zhang, T. W.; Xu, X. F.; Sun, J.; Wu, J. D.; Ying, Z. F.; Xu, N. *Mater. Sci. Eng., A* **2008**, *473*, 201.
- (9) Limpijumng, S.; Zhang, S. B.; Wei, S. H.; Park, C. H. *Phys. Rev. Lett.* **2004**, *92*, 155504.
- (10) Xu, N.; Xu, Y. L.; Li, L.; Shen, Y. Q.; Zhang, T. W.; Wu, J. D.; Sun, J.; Ying, Z. F. *J. Vac. Sci. Technol. A* **2006**, *24*, 517.
- (11) Wahl, U.; Rita, E.; Correia, J. G.; Marqurs, A. C.; Alves, E.; Soares, J. C. *Phys. Rev. Lett.* **2005**, *95*, 215503.
- (12) Malandrino, G.; Blandino, M.; Fregala, M. E.; Losurdo, M.; Bruno, G. *J. Phys. Chem. C* **2008**, *112*, 9595.
- (13) Hu, Z. G.; Li, W. W.; Wu, J. D.; Sun, J.; Shu, Q. W.; Zhong, X. X.; Zhu, Z. Q.; Chu, J. H. *Appl. Phys. Lett.* **2008**, *93*, 181910.
- (14) Hu, Z. G.; Li, Y. W.; Zhu, M.; Zhu, Z. Q.; Chu, J. H. *Appl. Phys. Lett.* **2008**, *92*, 081904.
- (15) Volbers, N.; Lautenschläger, S.; Leichtweiss, T.; Laufer, A.; Graubner, S.; Meyer, B. K.; Potzger, K.; Zhou, S. Q. *J. Appl. Phys.* **2008**, *103*, 123106.
- (16) Ghosh, C. K.; Malkhand, S.; Mitra, M. K.; Chattopadhyay, K. K. *J. Phys. D: Apply. Phys.* **2008**, *41*, 245113.
- (17) Hu, Z. G.; Li, Y. W.; Zhu, M.; Zhu, Z. Q.; Chu, J. H. *J. Phys. Chem. C* **2008**, *112*, 9737.
- (18) Jellison, G. E.; Boatner, L. *Phys. Rev. B* **1998**, *58*, 3586.
- (19) Yoshikawa, H.; Adachi, S. *Jpn. J. Appl. Phys., Part 1* **1997**, *36*, 6237.
- (20) Tompkins, H. G.; Irene, E. A. *Handbook of Ellipsometry*; William Andrew Publishing: Norwich, NY, 2005.
- (21) Djurišić, A. B.; Chan, Y.; Li, E. H. *Mater. Sci. Eng., R* **2002**, *38*, 237.
- (22) Hu, Z. G.; Li, W. W.; Li, Y. W.; Zhu, M.; Zhu, Z. Q.; Chu, J. H. *Appl. Phys. Lett.* **2009**, *94*, 221104.
- (23) Arslan, M.; Duymuş, H.; Yakuphanoglu, F. *J. Phys. Chem. B* **2006**, *110*, 276.
- (24) Bruna, M.; Borini, S. *Appl. Phys. Lett.* **2009**, *94*, 031901.
- (25) Hu, Z. G.; Strassburg, M.; Dietz, N.; Perera, A. G. U.; Asghar, A.; Ferguson, I. T. *Phys. Rev. B* **2005**, *72*, 245326.
- (26) Hu, Z. G.; Weerasekara, A. B.; Dietz, N.; Perera, A. G. U.; Strassburg, M.; Kane, M. H.; Asghar, A.; Ferguson, I. T. *Phys. Rev. B* **2007**, *75*, 205302.
- (27) Ye, J. D.; Tripathy, S.; Ren, Fang-Fang; Sun, X. W.; Lo, G. Q.; Teo, K. L. *Appl. Phys. Lett.* **2009**, *94*, 011913.
- (28) Wang, J. B.; Zhang, H. M.; Li, Z. F.; Lu, W. *Appl. Phys. Lett.* **2006**, *88*, 101913.
- (29) Yun, E. J.; Park, H. S.; Lee, K. H.; Nam, H. G.; Jung, M. *J. Appl. Phys.* **2008**, *103*, 073507.
- (30) Zeng, Y. J.; Ye, Z. Z.; Xu, W. Z.; Liu, B.; Che, Y.; Zhu, L. P.; Zhao, B. H. *Mater. Lett.* **2007**, *61*, 41.
- (31) Dai, L. P.; Deng, H.; Chen, J. J.; Wei, M. *Solid State Commun.* **2007**, *143*, 378.
- (32) Wang, Y. G.; Lau, S. P.; Lee, H. W.; Yu, S. F.; Tay, B. K.; Zhang, X. H.; Hng, H. H. *J. Appl. Phys.* **2003**, *94*, 354.
- (33) Studenikin, S. A.; Golego, N.; Cocivera, M. *J. Appl. Phys.* **1998**, *84*, 2287.
- (34) Ianno, N. J.; McConville, L.; Shaikh, N.; Pittal, S.; Snyder, P. G. *Thin Solid Films* **1992**, *220*, 92.
- (35) Wu, X. L.; Siu, G. G.; Fu, C. L.; Ong, H. C. *Appl. Phys. Lett.* **2001**, *78*, 2285.
- (36) Kwok, W. M.; Djurišić, A. B.; Leung, Y. H.; Chan, W. K.; Phillips, D. L. *Appl. Phys. Lett.* **2005**, *87*, 223111.
- (37) Herzinger, C. M.; Johs, B.; McGahan, W. A.; Woollam, J. A.; Paulson, W. *J. Appl. Phys.* **1998**, *83*, 3323.
- (38) Adachi, S. *Phys. Rev. B* **1987**, *35*, 7454.
- (39) Adachi, S. *Phys. Rev. B* **1988**, *38*, 12345.
- (40) Bahng, J. H.; Lee, M.; Park III, H. L.; Kim, W.; Jeong, J. H.; Kim, K. J. *Appl. Phys. Lett.* **2001**, *79*, 1664.
- (41) Press, W. H.; Teukolsky, S. A.; Vetterling, W. T.; Flannery, B. P. *Numerical Recipes in C: The Art of Scientific Computing*; Cambridge University Press: Cambridge, MA, 1992.
- (42) Cardona, M. *Phys. Rev.* **1965**, *140*, A651.
- (43) Kim, K. J.; Park, Y. R. *Appl. Phys. Lett.* **2002**, *19*, 1420.
- (44) Washington, P. L.; Ong, H. C.; Dai, J. Y.; Chang, P. H. *Appl. Phys. Lett.* **1998**, *72*, 3261.
- (45) Postava, K.; Sueki, H.; Aoyama, M.; Yamaguchi, T.; Ino, Ch.; Igasaki, Y. *J. Appl. Phys.* **2000**, *87*, 7820.
- (46) Bruggeman, D. A. G. *Ann. Phys. (Leipzig)* **1935**, *24*, 636.
- (47) Fujiwara, H.; Koh, J.; Rovira, P. I.; Collins, R. W. *Phys. Rev. B* **2000**, *61*, 10832.

JP902766A